Applied Thermal Engineering 247 (2024) 123070

Contents lists available at ScienceDirect

Applied Thermal Engineering

journal homepage: www.elsevier.com/locate/apthermeng

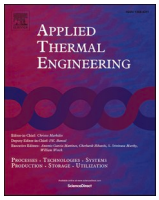

Research Paper

Optimizing R152a/R600 and R290/R600 mixtures for superior energy performance in vapor compression systems: Promising alternatives to Isobutane (R600a)

Daniel Calleja-Anta *, Manel Martínez-Ángeles, Laura Nebot-Andres, Daniel Sánchez, Rodrigo Llopis

Thermal Engineering Group, Mechanical Engineering and Construction Department, Jaume I University, Spain

ARTICLE INFO

Keywords:
Domestic refrigeration
R600a alternatives
R152a/R600
R290/R600
Refrigerant mixtures
Energy efficiency

ABSTRACT

This study presents an experimental investigation into the optimal composition of R152a/R600 and R290/R600 mixtures as potential alternatives to isobutane (R600a) in a single-stage vapor compression cycle. The research involved testing eight different mass compositions for R152a/R600 and ten mass compositions for R290/R600, comparing their performance with that of R600a. After careful analysis, the "optimum" mass compositions were identified as (10/90)% for both R152a/R600 and R290/R600, achieving a balanced trade-off among coefficient of performance (COP), volumetric cooling capacity (VCC), and cooling output ($\dot{Q}_o$). Further tests were conducted on the "optimum" compositions at nine different secondary fluid temperature inlets. The results indicated an average COP increase of + 7.3 % for the R152a/R600 mixture, with decreases of −11.4 % in VCC and −9.7 % in $\dot{Q}_o$. Similarly, the R290/R600 (10/90)% mixture showed a COP increase of + 10.3 %, accompanied by VCC and $\dot{Q}_o$ decreases of −8.8 % and −6.6 %, respectively. Notably, both mixtures exhibited superior energy performance compared to isobutane while maintaining similar thermodynamic properties, particularly the R290/R600 (10/90)% mixture. These findings suggest that the R152a/R600 and R290/R600 mixtures could serve as long-term, high-efficiency alternatives to R600a in vapor compression cycles.

1. Introduction

In the realm of low cooling capacity refrigeration applications, it is possible to distinguish between two subsectors: the domestic subsector, primarily consisting of refrigerators and freezers, and the commercial subsector formed by sealed equipment. Both of these subsectors were significantly impacted by the implementation of European Regulation No. 517/2014 (European [1], which imposed restrictions on the use of refrigerants with a maximum GWP of 150, being effective from the beginning of 2015 for the domestic sector and from the start of 2022 for the commercial one.

While it might appear that the low cooling capacity refrigeration sector does not require extensive research efforts to enhance its efficiency due to its low unitary energy consumption, it is essential to note that, according to the UNEP, [2], the domestic subsector alone sees an annual production of around 170 million refrigerators and freezers. In 2018, the total number of units in use within this subsector ranged between 2 billion and 2.3 billion, collectively consuming approximately 4 % of the world's electric energy.

Since the early 2000 s, there has been a notable adoption of R-600a (isobutane) as the predominant refrigerant in the low-power refrigeration sector in Europe, and this trend has been steadily growing in other regions of the world as well. In 2018, it was estimated that out of the 170 million units produced annually, approximately 100 million were already being manufactured with isobutane (UNEP, 2018). Considering the upward trajectory observed until that year and the regulatory updates that have made the use of flammable refrigerants more flexible (such as the IEC 60335–2-89: 2019, which increased the flammable refrigerant charge in commercial equipment from 150 g to 500 g for A3 refrigerants and to 1200 g to A2 and A2L ([3]) it is highly likely that this percentage has increased significantly in recent years.

R-600a replaced R-134a in these applications mainly due to the efforts to combat climate change. According to the 6th IPCC Assessment Report [4], R-134a has a Global Warming Potential (GWP) of 1530, whereas R-600a's GWP is nearly negligible (3). In addition to the

* Corresponding author.
E-mail address: calleja@uji.es (D. Calleja-Anta).

https://doi.org/10.1016/j.applthermaleng.2024.123070
Received 8 November 2023; Received in revised form 7 March 2024; Accepted 29 March 2024
Available online 30 March 2024

Nomenclature

ATS	Auxiliary Thermal System
c_p	specific heat at constant pressure, $kJ \cdot kg^{-1} \cdot K^{-1}$
COP	Coefficient of Performance
C_r	Compression rate
GWP	Global Warming Potential over 100-year, $kg_{co2,eq}$ / kg_{ref}
h	specific enthalpy, $kJ \cdot kg^{-1}$
HX	Heat Exchanger
m	mass flow rate, $kg \cdot s^{-1}$
M	Molar mass, $g \cdot mol^{-1}$
MAE	Mean Absolute Error
NBP	Normal Boiling Point, °C
p	absolute pressure, bar
$\dot{P}_c$	compressor power consumption, W
$\dot{Q}_o$	cooling capacity, W
$\dot{q}_o$	specific cooling capacity, $kJ \cdot kg^{-1}$
RH	Relative Humidity,%
t	temperature, °C
V	volume flow rate, $L \cdot s^{-1}$
VCC	Volumetric Cooling Capacity, $kJ \cdot m^{-3}$
x_v	vapor tittle

Subscripts

suc	refers to compressor suction conditions
crit	at critical conditions
dis	refers to compressor discharge conditions
exp	refers to the expansion device
gly	refers to propylene glycol–water mixture
in	inlet
k	related to condensation
o	related to evaporation
out	outlet
pc	refers to the phase change
ref	related to the refrigerant
sec,fluid	related to the secondary fluid
w	related to the water

Greek symbols

λ	latent heat of phase change, $kJ \cdot Kg^{-1}$
Ø	diameter, cm

reduction of emissions of direct origin, the indirect reduction must also be taken into account, since it is estimated that the energy reductions provided by isobutane with respect to R-134a are 5 %, according to different authors and in different applications. For instance, Rasti et al. [5] conducted tests using a domestic refrigerator and found that energy savings with R-600a compared to R-134a were 7 % with the original compressor and reached 18.7 % when using a compressor designed specifically for isobutane. In a separate study, Sánchez et al. [6] conducted 16-hour tests comparing several pure refrigerants as substitutes for R-134a, using specific compressors with the displacement adjusted for each of them in a beverage cooler, where isobutane showed an energy reduction of 1.2 %.

In addition to reducing environmental impact, isobutane offers several advantages over other refrigerants. One notable advantage is the lower operating pressure of isobutane compared to most commercial refrigerants. The pressure levels at which it works are lower than most commercial refrigerants, which helps to create exchangers that require less robustness and therefore are significantly cheaper than refrigerants operating at higher pressures [7]. Another positive side effect related to the pressures is the reduction of noise, which in domestic installations is an important parameter; and the reduction of peak electrical power required at the beginning of the compression process, lower requirement of installed power and fewer electrical windings in the compressor [8]. These combined benefits make isobutane an attractive choice in various refrigeration applications.

However, previous to the adoption of the isobutane, several refrigerants were evaluated as potential alternatives. These candidates, however, often had drawbacks or failed to match the advantages offered by R-600a. For instance, R-1234yf and R-1234ze(E) boast an A2L flammability classification [9], but they are synthetic refrigerants with higher operating pressures compared to isobutane. Moreover, certain studies have reported energy performance that is similar to or even worse than R-134a when using these alternatives. Aprea et al. [10] addressed the possibility to do a R-600a drop-in replacement with the R-1234yf, obtaining higher condensation pressures, increment of the cooling capacity and 3 % of energy savings. Similarly, in a complementary study conducted with other domestic appliance, Aprea et al. [11] demonstrated energy reductions when using the R-1234ze(E) respect to R-134a of 9 %. Sánchez et al. [8] also studied these two refrigerants in a single-stage vapor compression plant reporting COP reductions between 8.3 % and 11 % for R-1234yf and between 2.8 % and 13 % for R-1234ze(E). These reductions were accompanied by cooling capacity decreases of 4.5 % to 8.6 % for R-1234yf and 23.1 % to 26.6 % for R-1234ze(E). R-152a (also a synthetic refrigerant) has also been examined as a potential alternative for domestic refrigeration. Bolaji [12] conducted an investigation into its use in a domestic refrigerator, where they observed COP increases of 4.7 % and energy consumption reductions of 4 %. Similarly, Maiorino et al. [13], using a similar experimental system, demonstrated energy reductions of up to 7.4 % and an 8 % decrease in the time required for pull-down in a commercial refrigerator.

Refrigerant blends have also been the subject of study and debate. In the study mentioned earlier by Rasti et al. [5], the R-436A mixture (46 % R-600a and 54 % propane) was examined, resulting in energy reductions of up to 14.6 %, lower than those achieved with isobutane. In a different study, Mohanraj et al. [14] tested a mixture consisting of 45.2 % R-290 and 54.8 % R-600a in a domestic refrigerator, achieving energy reductions of 11.1 % compared to isobutane, being a potential alternative.

Isobutane has emerged as the standard choice among alternatives due to its numerous advantages. However, there is a potential possibility for improving its energy characteristics while retaining its benefits at the same time by developing refrigerant blends with thermodynamic properties similar to R-600a.

This research direction was initially explored by Calleja-Anta et al. [15], through a thermodynamic screening process. 55,440 possible ternary mixtures were theoretically analyzed to identify those with higher COP than isobutane, similar Volumetric Cooling Capacity (VCC), discharge temperatures, effective evaporator glide below 10 K, and a GWP lower than 150. The study revealed several promising binary mixtures primarily composed of butane (R-600) and a secondary refrigerant. These mixtures were supposed to offer COP increases ranging from 8.6 % to 1.7 %, with VCC reductions between 28.4 % and 8.2 %. The most favorable mixtures featured the refrigerant pairs R-1270/R-600, R-152a/R-600, R-1234zeE/R-600, and R-290/R-600, with varying compositions depending on boundary conditions, but generally consisting of around 90 % butane by mass proportion.

Building on this foundation, subsequent research in 2022 [16] involved drop-in tests of some previously identified mixtures in a domestic refrigerator over a 24-hour period to verify energy savings. At optimized charges, the mixture R-1234yf/R-600a (7.5/92.5)% achieved an energy reduction of 2.15 % compared to R-600a, R-1234ze(E)/R-600 (10.5/89.5)% achieved a reduction of 3.84 %, and R-290/R-600 (11/

89)% exhibited a reduction of 1.31 %, all while maintaining similar or even lower operating pressures and with similar duty cycles.

The potential for enhancing the energy performance of isobutane through mixtures was further explored in a recent study by Calleja-Anta et al. [17]. Experimental tests were conducted in a stand-alone commercial refrigeration cabinet over 16 h, with the capability to adapt its operation to the tested refrigerants. Two of the tested mixtures, R-1234ze(E)/R-600 (8/92)% and R-152a/R-600 (8/92)%, achieved energy reductions of 2.69 % and 5.04 %, respectively, compared to R-600a.

Nonetheless, these previous studies had certain limitations. The mass compositions were optimized based on simplified theoretical models, which allowed for predictions regarding the behavior of a large number of mixtures. However, these models did not account for critical factors such as heat transfer and compressor performance. Furthermore, the experimental setups used did not facilitate a comprehensive thermodynamic analysis of the mixtures.

The objective of the present work is to perform an experimental optimization of the composition of the mixtures R-152a/R-600 and R-290/R-600, two of the mixtures that have shown a better energetic performance in the previous studies. To achieve this, experiments using varying composition proportions of these two mixtures have conducted within a single-stage vapor compression bench. This experimental setup was developed and fully monitored, allowing to measure key parameters including COP, VCC and $\dot{Q}_o$. The objective is to identify the "optimum" composition that achieves the most favorable balance among these three parameters.

It is important to note that the goal here is not to find a mixture that can directly replace isobutane (drop-in) but rather to identify a mixture that can enhance the overall energy performance of R-600a while preserving the advantages previously described. This research also features a novel heat exchanger design to facilitate the measurement of the refrigerant's internal evolution during the phase-change process.

2. Methods and materials

This section describes the thermodynamic properties of the considered refrigerants, the experimental plant used to perform the tests, the measurement system and the methodology followed.

2.1. Fluids and mixtures

Table 1 presents the properties of the four refrigerants considered in this study. Notably, the only refrigerant that exceeds the limit of GWP of 150 is R-152a, but it will be used in proportions whose resulting GWP will be below this threshold. Comparing butane and isobutane, butane exhibits a higher Normal Boiling Point (NBP), critical temperature (t_{crit}), and critical pressure (P_{crit}) than isobutane. The increased NBP correlates with a lower evaporation pressure required to achieve a similar evaporation temperature. Furthermore, butane demonstrates a significantly higher latent heat of phase change (+10.88 % at 40 °C and + 7.74 %) and suction specific volume (+57.83 %) in comparison to isobutane. On the other hand, both R-152a and R-290, which will be combined with R-600 to form the mixtures, exhibit lower NBPs, t_{crit}, and P_{crit} than isobutane. Specifically, R-152a has a lower latent heat of phase change compared to the base refrigerant (-16.57 % at −40 °C and −12.79 % at −10 °C), while R-290 shows a similar latent heat at −40 °C (-1.41 %) and a higher latent heat at −10 °C (+6.82 %). The properties of the resulting mixtures, formed by mixing butane with R-152a and R-290, are expected to fall within the range of properties exhibited by each individual refrigerant, depending on the proportion of each fluid in the mixture.

Table 1
Physical and environmental characteristics of the 4 refrigerants involved in this work (obtained with Refprop 10 [18].

	R-600a	R-600	R-152a	R-290
M (g·mol-1)	58.1	58.1	66.1	44.1
NBP (°C)	−11.8	−0.5	−24.0	−42.1
t_{crit} (°C)	134.7	152	113.3	96.7
p_{crit} (°C)	36.2	37.9	45.2	42.5
λ at **t** = 40 °C (kJ·kg^{-1})	311.5	345.4	259.9	307.1
λ at **t** = -10 °C (kJ·kg^{-1})	363.5	394.0	317.0	388.3
v_{suc} at **t** = -10 °C & x_v = 1 (m^3·kg-1)	0.332	0.524	0.171	0.131
$GWP_{100\text{-years}}$ [4]	3	3	164	3

2.2. Description of the experimental plant and measurement system

The test bench where the experimental tests are performed is represented through its refrigeration diagram in Fig. 1. It is a single-stage vapor compression cycle, using a variable speed hermetic reciprocating compressor, a condenser, a liquid vessel of 1.2 L that could be bypassed if needed, an expansion valve (whose driver can be configurable to work accordingly with each mixture) and an evaporator. Table 2 shows the characteristics of the main elements.

The compressor chosen is a variable speed hermetic reciprocating one, with the characteristics shown in Table 2. We control the compressor speed using a wave generator instead of the manufacturer driver.

The geometry of the evaporator and condenser is based on a tube-in-tube configuration, as can be seen in Fig. 2. The secondary fluid flows through the outer tube while the refrigerant through the inner one, counter current. The heat exchangers (HX) are made with a system of elbows and "T" in which the refrigerant tube passes through the secondary fluid tube different times, with a length of 23.5 cm each step. The condenser has 16 refrigerant-water pitches, while the evaporator has 14. At each pass the inner and outer tube were ensured to be concentric, as shown in Fig. 2, right.

The selection of this particular geometry for the heat exchangers was motivated by the desire to establish a configuration that is both simple and readily accessible, in which the total heat exchange area was easy to be measured and were able the integration of sensors at various key locations, as explained in the following paragraphs.

To absorb the heat power generated by the condenser and provide thermal load to the evaporator, two auxiliary thermal systems (ATS) were installed. They consist of a loop with circulating secondary fluid, in which its inlet temperature is controlled by a PID controller. Distilled water was used for the condenser loop while a mixture of propylene glycol and water (50/50 %$_v$) was used for the evaporator one.

In order to capture the various thermodynamic states experienced by the refrigerant throughout the cycle, the plant was instrumented with different sensors all along the installation, whose location is shown in Fig. 1. 6 pressure gauges (P) were installed [3 high-pressure (1–30 bar), 1 medium-pressure (0–16 bar) and 2 low-pressure (0–9 bar)]. 36 T-type thermocouples (T) were installed to measure the refrigerant temperatures. 32 of the refrigerant thermocouples were aimed to measure the evolution of the refrigerant temperatures through the two heat exchangers, placed as immersion thermocouples at the outlet of each step of 23.5 cm of pipe in which there is heat exchange between the refrigerant and the secondary fluid (see Fig. 2, center). In that way, 16 thermocouples were installed at the condenser and 15 in the evaporator. 4 additional surface thermocouples were placed in different points of the cycle (suction, discharge, liquid vessel outlet and expansion valve inlet). The uncertainty of the T-thermocouple is of ± 0.5 K and of the pressure gauges is of ± 1 % of the full measuring range. A Coriolis mass-flow meter was installed at the compressor outlet with an accuracy of ± 0.15 % of the measurement. To measure the electric power demanded, a digital wattmeter was used with an uncertainty of ± 0.5 % of measurement.

The loops with secondary fluids were also equipped with 18 surface T-type thermocouples (W) to measure the evolution of the fluid temperature at different points (9 in each HX, with 3 thermocouples at the inlet, 3 at the outlet and 3 more at the indicated points). One mass-flow

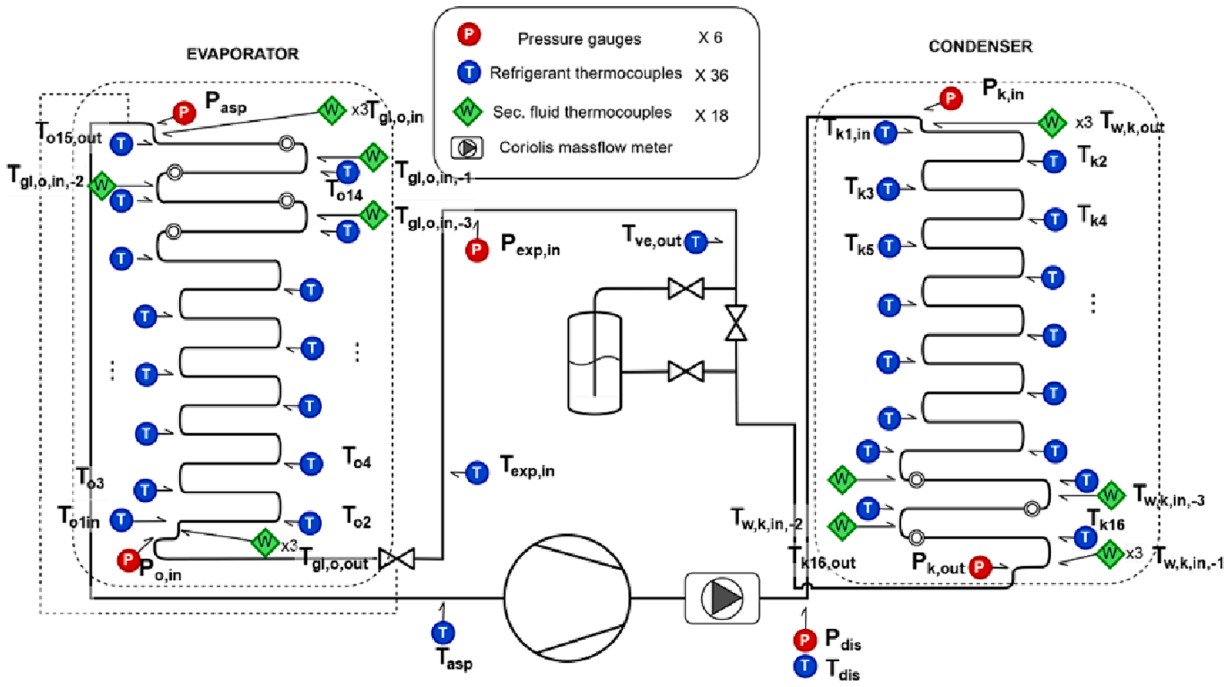

Fig. 1. Diagram of the plant with the position of the sensors installed and their names.

Table 2
Characteristics of the main elements of the refrigeration circuit.

Element	Characteristics
Compressor	R600a Variable speed hermetic reciprocating compressor Displacement: 11.14 cm^3, 1/4 horsepower, LBP. Speed can be adjustable from 1300 RPM to 4500 RPM. Model: EMBRACO VES D11C.
Condenser	Tube-in-tube heat exchanger, self-made. Countercurrent flow. 16 steps per 23.5 cm pipe. Outer tube intended for water flow. $Ø_i = 16$ mm. Inner tube intended for refrigerant flow. Ø = ¼". Thickness = 0.8 mm. Total heat exchange area = 750 cm^2
Electronic valve	Used as thermostatic expansion valve. Driver configurable to each refrigerant mixture with bubble and dew temperatures.
Evaporator	Tube-in-tube heat exchanger, self-made. Countercurrent flow. 14 steps per 23.5 cm pipe. Outer tube intended for water flow. $Ø_i = 16$ mm. Inner tube intended for refrigerant flow. Ø = 3/8". Thickness = 0.8 mm. Total heat exchange area = 984.5 cm^2

meter was installed at the evaporator loop and one volumetric-flow meter at the condenser one, with uncertainties of ± 0.55 % and ± 2.1 % respectively.

The plant was conveniently thermally insulated and placed in a climatic chamber with control of the temperature.

2.3. Experimental procedure

One of the objectives of this study is to determine experimentally the "optimum" composition of the binary mixtures R-152/R-600 and R-290/R-600 which can be used as R-600a alternatives. To achieve this objective, the mixtures were evaluated in a bench test at varying compositions in order to identify the composition that provides the best balance between the COP, VCC and the $\dot{Q}_o$ relative to isobutane.

The "optimum" composition was selected in base of a commitment between COP, VCC $\dot{Q}_o$ in comparison to R-600a, as in the following sections will be seen.

To obtain the "optimum" composition of each mixture, different compositions were tried, starting from 97.5 % in mass basis of R-600 and 2.5 % of the other refrigerant. The composition of the second refrigerant was incremented in steps of 2.5 % until one "optimum" was reached. Also, tests were conducted with pure butane (R-600) as well as with R-600a, which will be used as the reference. Between each composition tested, a complete vacuum of the refrigeration plant was done and then the plant was charged accordingly with each composition. Firstly, the plant was charged directly from the R-600 bottle (as it is the fluid with less NBP and since with less pressure) and later with the correspondent charge of the second fluid. The plant was tested with the liquid vessel open to avoid that different refrigerant charges could affect in the overall operation of the plant, fluctuating all refrigerant charges between 141 g and 160 g. A weight scale with a ± 0.5 g of uncertainty was used and all the fluids used were certified with 99.5 % of purity. For each composition, the electronic expansion valve of the evaporator was adapted to work with each mixture, configuring the controller according to the bubble and dew temperatures of each mixture (evaluated with REFPROP). This optimization process was repeated twice, being the average parameters of each compositions the one used to analyze.

The optimization process was conducted maintaining the same inlet secondary fluid temperatures and secondary fluid mass flows for all the tests. The water loop intended for condenser was set at an inlet temperature of 30 °C ± 0.8 °C and a mass flow of 90 $kg{\cdot}h^{-1}$ ± 0.42 $kg{\cdot}h^{-1}$, while the inlet conditions for the loop dedicated for the evaporator was 0 °C ± 0.06 °C and 80 $kg{\cdot}h^{-1}$ ± 0.85 $kg{\cdot}h^{-1}$.

Once the "optimum" composition was chosen, the plant was again subjected to another vacuum and recharge with the selected proportions to analyze their performance under different inlet secondary fluid temperatures. Three inlet loop condenser temperatures (25 °C, 30 °C and 35 °C) and three different inlet loop evaporator temperatures (-5 °C, 0 °C and 5 °C) were tested, resulting in a total of 9 tests. R-600a was also tested under these conditions as reference. During this process, the rest of parameters were maintained as in the optimization process.

All the experimental tests described were performed with a useful superheating of expansion valve set at 8 K and with the compressor speed set at 4500 RPM. The selected period to be tested was 8 min, once steady-state conditions were clearly reached. To maintain constant the

Fig. 2. Different pictures of the test bench before the application of heat insulation. From left to right: a general picture of the machine, followed by a focused view of the condenser, and finally, the cross section of the evaporator.

energy losses with the environment, the experimental unit was placed inside a climatic chamber with a temperature of 25 °C, which was measured with a thermohydrometer with an accuracy of ± 2 % RH and ± 0.2 K.

3. Data validation and discussion of the calculation methodology

In this section, the data validation process and the discussion of the calculation methodology are addressed.

The data validation is conducted in both the condenser and the evaporator for the 9 different tests of isobutane that were performed under varying inlet secondary fluid temperature conditions, as explained in the previous section. Validation consists of checking the heat transfer in evaporator and condenser of refrigerant and secondary fluids.

The heat power absorbed by the secondary fluid circuits ($\dot{Q}_{sec,fluid}$) is calculated according to Eq. (1), where $\dot{m}_{fluid,sec}$ is the mass flow rate, c_p is the specific heat at constant pressure and Δt the temperature difference between the inlet and outlet of the heat exchanger. c_p of the water-propylene glycol mixture is calculated according with Conde [19].

$$\dot{Q}_{secfluid} = \dot{m}_{secfluid} \cdot c_p \cdot \Delta t \tag{1}$$

Eqs (2) to (4) are used to calculate the heat power absorbed by the refrigerant in the evaporator ($\dot{Q}_{o,ref}$), in this study. The enthalpy value at the outlet of the evaporator ($h_{o,out}$) is determined as a function of the suction pressure and temperature. The inlet enthalpy ($h_{o,in}$) is determined as a function of the measured pressure with the gauge positioned before the expansion valve and the temperature prior to the valve, isenthalpic lamination is considered.

$$\dot{Q}_{o,ref} = \dot{m}_{ref} \cdot (h_{o,out} - h_{o,in}) \tag{2}$$

$$h_{o,out} = f(p_{asp},\ t_{asp}) \tag{3}$$

$$h_{o,in} = f(p_{exp,in},\ t_{exp,in}) \tag{4}$$

Similarly, the heat power rejected by the refrigerant in the condenser ($\dot{Q}_{k,ref}$) is calculated using Eqs (5) to (7), in which the inlet condenser enthalpy is function of the discharge pressure and the inlet condenser temperature (measured with the first immersion thermocouple in the condenser) and the outlet enthalpy is calculated with the value of the pressure gauge and the outlet condenser temperature (last immersion thermocouple).

$$\dot{Q}_{k,ref} = \dot{m}_{ref} \cdot (h_{k,in} - h_{k,out}) \tag{5}$$

$$h_{k,in} = f(p_{dis},\ t_{k,in}) \tag{6}$$

$$h_{k,out} = f(p_{k,out},\ t_{k,out}) \tag{7}$$

Fig. 3 displays the results obtained from the 9 tests conducted with isobutane, indicating the inlet temperature secondary fluid of each test. To evaluate the acceptability of the results, a discrepancy tolerance of ± 6 % between the two calculations considered adequate. All values obtained are inside this acceptable range. In the condenser, deviations observed across all tests remain below 3 % (with the exception of the "35 °C, −5°C" test, which exhibits a 4.65 % deviation). In the evaporator, deviations tend to be more pronounced when the inlet temperature of the secondary fluid is lower. The deviation reaches approximately 5 % at an inlet temperature of −5°C, around 3.5 % at 0 °C, and approximately 0.5 % at 5 °C.

Based on the obtained results, it can be concluded that the level of agreement achieved between the calculations conducted from the two distinct perspectives is considered satisfactory.

However, in contrast with isobutane, a less optimal agreement was observed in the tests conducted with the remaining mixtures when performing heat balances between the data obtained from the refrigerant and the secondary fluid. Fig. 4 shows the data validation of all the tests performed with the mixtures R-152a/R-600 and R-290/R-600 at different mass compositions and different temperature inlet secondary fluid temperatures. This discrepancy between both calculations occurs principally with the mixture R-290/R-600, exhibiting differences higher than ± 6 % for 8 of the tests in the condenser and for 11 in the

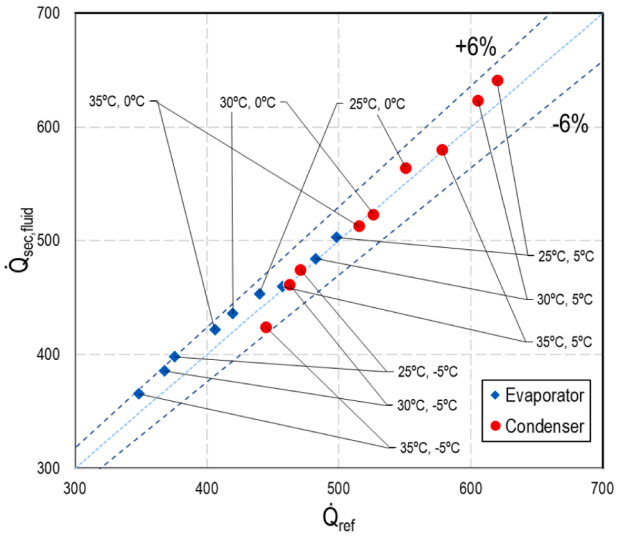

Fig. 3. Data validation for the isobutane tests. The inlet secondary fluid temperature for each test is indicated, being the first value the one related to the condenser and the second value the evaporator.

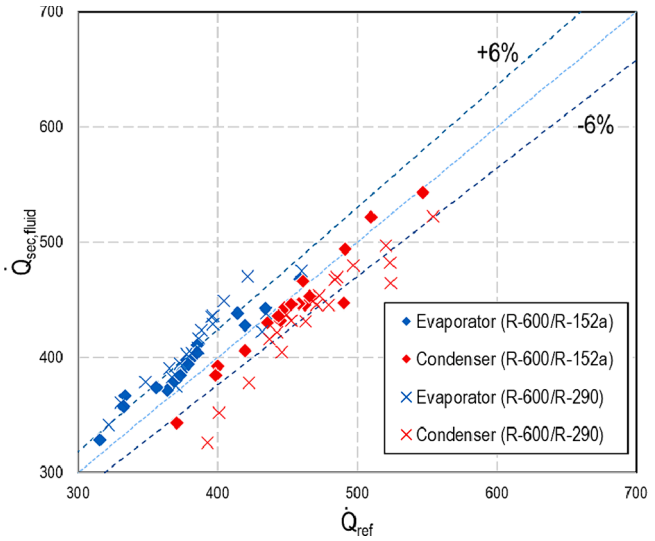

Fig. 4. Heat exchange of the all the tests performed with the mixtures R-152a/R-600 and R-290/R-600, with different mass compositions and different secondary fluid inlet temperatures.

evaporator of a total of 20 tests considered. According to the authors' perspective, these variations can be attributed to uncertainties and inaccuracies inherent to the thermodynamic property calculations of new mixtures.

The assumption done by the authors is reinforced by the comparison of the PT curves obtained by REFPROP 10 and the saturation points obtained experimentally as shown in Fig. 5. The figure represents with a solid line the saturation curves of the isobutane and the two mixtures with the "optimum" composition, as seen in the following sections. For each fluid, a total of 9 tests are available at different operating temperatures conditions. In the case of the two mixtures, a liquid saturation line and a vapor one can be differentiated, due to the existing glide. The data points in the figure represent the pressure–temperature values obtained experimentally, measured from points known to be in saturation conditions. The condenser and evaporator are both equipped with thermocouples, with 16 and 15 thermocouples respectively. This instrumentation enables the identification of the points where the phase change begins, as seen in following sections. Generally, in the condenser, the process begins at the 3rd thermocouple and concludes at the 16th thermocouple, while in the evaporator, the 12th thermocouple indicates the start of superheating. The corresponding pressures for these points are $p_{k,in}$, $p_{k,out}$ and p_{asp}, respectively. Furthermore, as isobutane does not exhibit glide, it is possible to represent the points of the evaporator inlet, which are measured by the 1st thermocouple in the evaporator, along with the pressure $p_{o,in}$.

The comparison between the experimental data obtained with isobutane and the theoretical saturation curves provided by REFPROP 10 reveals a good agreement. The mean absolute error (MAE) between the experimental values and the predicted ones is 0.5 K, which is considered a favorable approximation and falls within the range of sensor uncertainties. Furthermore, the observed trend aligns well with the theoretical curves.

However, the comparison of the saturation states for the mixtures between the experimental data and the predictions obtained with REFPROP 10 is not as favorable. For the mixture R-152a/R-600 (10/90)%, the MAE is calculated to be 1.43 K (0.82 K for the saturated liquid curve and 1.73 K for the vapor curve). Similarly, for the mixture R-290/R-600 (10/90)%, the MAE is found to be 1.9 K (1.89 K for the liquid curve and 2.01 K for the vapor curve).

The findings presented in Fig. 4 and Fig. 5 indicate a strong agreement between the calculated parameters obtained with REFPROP 10 and the data acquired through various sensors for R-600a. However, this agreement does not hold true for the two alternative mixtures tested. This observation leads to two significant conclusions: i) the calibration of the plant is considered adequate since the results obtained data from the sensors present in the plant for isobutane, align well with the provided by REFPROP, which are known to be reliable; ii) the data obtained for the mixtures does not correspond to the data predicted by REFPROP. This suggests that parameters obtained through direct measurements (collected from various sensors throughout the plant) are more reliable compared to indirect parameters that involve calculations utilizing REFPROP, as it necessitates the utilization of mixing rules, which are based on estimations [20].

Overall, these findings highlight the importance of relying on direct measurements when possible for increased reliability in the determination of parameters, as opposed to relying solely on calculations involving REFPROP and its associated mixing rules. It is worth noting that the authors have adjusted the mixing coefficients for each mixture to the most recent coefficients available in the bibliography [21], but not a significant improvement was observed.

4. Composition optimization process - thermodynamic analysis

4.1. Composition optimization process

As previously mentioned, the "optimization" process involves conducting tests on a range of mass compositions within the mixture. This range starts from 97.5 % butane (with 2.5 % of the second fluid) and progresses incrementally in 2.5 % intervals until an "optimum" composition is determined. Throughout these tests, a constant inlet secondary fluid temperature of 30 °C is maintained for the condenser (with a secondary fluid mass flow rate of 90 kg·h^{-1}), while an inlet temperature of 0 °C is maintained for the evaporator (with a mass flow rate of 80 kg·h^{-1}).

The selection of the "optimum" composition is based on the evolution of the COP, VCC and $\dot{Q}_o$ parameters. These two parameters are calculated through the secondary fluid [Eq.(1)], since yields satisfactory precision for the purpose of this work.

The COP is calculated according to Eq.(8), considering the cooling capacity as the heat absorbed by the evaporator loop ($\dot{Q}_{o,secfluid}$) and the power consumption of the compressor ($\dot{P}_c$). VCC is determined using Eq.

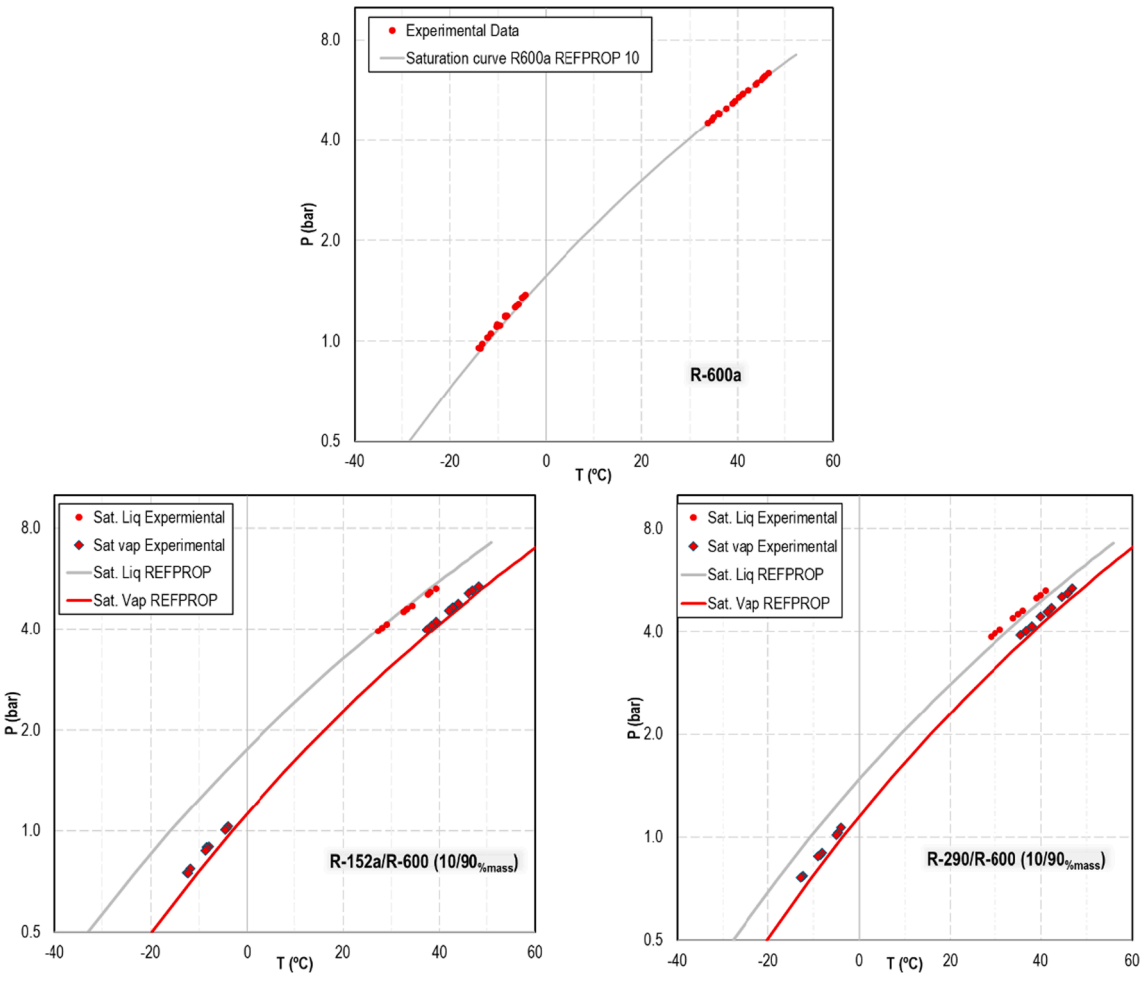

Fig. 5. Comparison of saturation curve values obtained by REFPROP 10 (solid lines) and experimental saturation values for each fluid (points).

(9), which considers the specific cooling capacity and the specific suction volume (v_{asp}^{*}), which is calculated with REFPROP, as there are no direct measurements available for this parameter.

$$COP = \frac{\dot{Q}_{o,secfluid}}{\dot{P}_c} \tag{8}$$

$$VCC = \frac{\dot{q}_{o,secflud}}{v_{asp}^{*}} = \frac{\frac{\dot{Q}_{o,secfluid}}{\dot{m}_{ref}}}{v_{asp}^{*}} \tag{9}$$

Fig. 6, Fig. 7 and Fig. 8 depict the evolution of the COP, the VCC and the cooling capacity of the two alternative mixtures analyzed in this work as the proportion of the less dominant refrigerant increases while the proportion of butane decreases. In a red line the isobutane value (considered the reference) is represented. Isobutane presents a COP of 2.51 a VCC of 827.4 kJ·m^{-3} and a $\dot{Q}_o$ of 435.9 W. Pure butane presents values of 2.74, 640.4 kJ·m^{-3} and 366.25 W respectively.

The COP evolution of the two analyzed mixtures differs significantly between the two mixtures. The mixture consisting of refrigerants R-152a

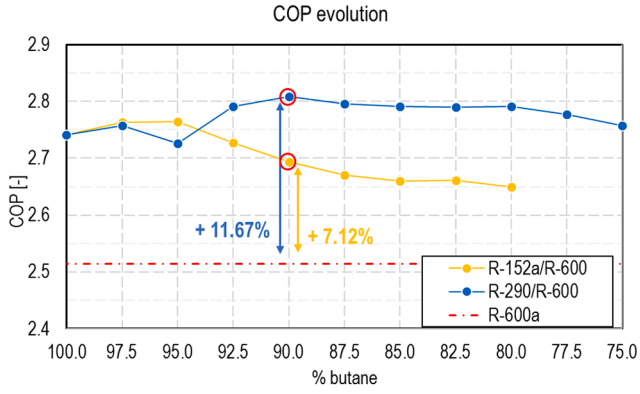

Fig. 6. Evolution of the COP when varying the composition of the alternative mixtures. The COP obtained with isobutane is represented by the red line.

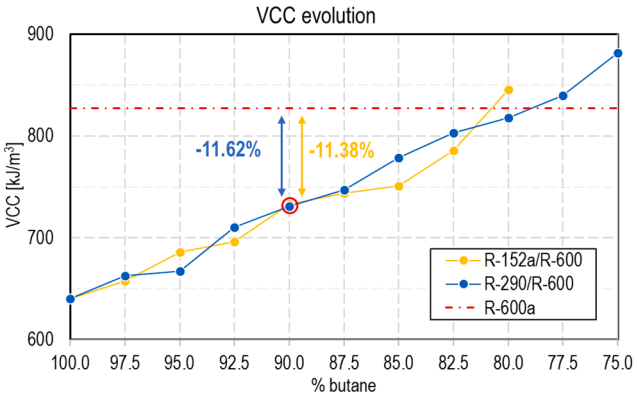

Fig. 7. Evolution of the VCC when varying the composition of the alternative mixtures. The VCC obtained with isobutane is represented by the red line.

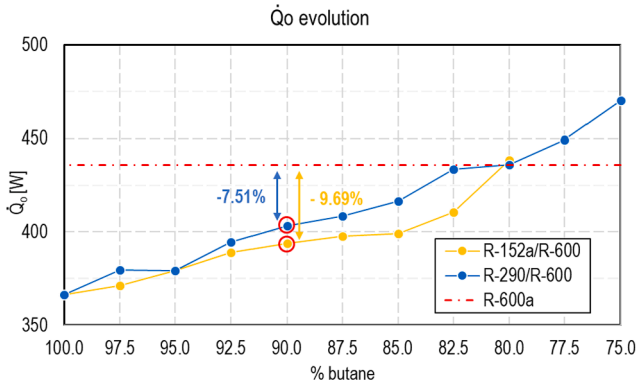

Fig. 8. Evolution of the cooling capacity when varying the composition of the alternative mixtures. The cooling capacity obtained with isobutane is represented by the red line.

and R-600 exhibits the highest COP values at compositions of 2.5/97.5 % and 5/95 % (2.76), followed by a slight but noticeable decrease as the R-152a composition increases. On the other hand, the mixture R-290/R-600 achieves its maximum COP at a composition of 10/90 % (2.81), maintaining a similar value until the proportion reaches 20/80 %, after which it starts to decrease.

Regarding the evolution of VCC, it is evident that both mixtures exhibit a similar trend. As anticipated, pure butane demonstrates a considerably lower VCC compared to isobutane (–22.77 %). This difference arises because, despite having a greater enthalpy difference, the specific volume at the compressor inlet is significantly lower for butane, as detailed in Table 1. As the proportion of the secondary refrigerants increases, it is observed that the VCC rises. This is due to the fact that secondary refrigerants have higher densities than butane, leading to a rapid reduction in the specific volume at the compressor inlet, subsequently increasing the VCC. The recorded values for both mixtures remain similar across the entire mass range tested and surpass those of isobutane proportions of R-152a exceed 20 % and R-290 surpasses 77.5 %.

The trend in the evolution of cooling capacity closely mirrors that of Volumetric Cooling Capacity, with the key distinction being that the mixture containing propane consistently exhibits higher values across the entire mass range. Similarly to the VCC, the $\dot{Q}_o$ increases as the density of the mixture increases. In both mixtures, cooling capacity surpasses the value of isobutane when the proportion of the secondary fluid exceeds 20 %.

It is worth noting that throughout the entire range of compositions examined, both mixtures present an A3 flammability classification, according with Calleja-Anta et al. [22] considering the fractionation in the classification.

The “optimum” composition for the mixtures has been determined by carefully considering the trade-offs among the three discussed parameters. For the R-152a/R-600 mixture, the composition selected as the most advantageous is 10/90 %. Lower proportions of R-152a result in a significant reduction in VCC compared to isobutane (-15.8 % at 7.5/92.5 % versus −11.4 % for the chosen composition), while higher proportions do not yield substantial improvements (-10.1 % at 12.5/87.5 %). At the selected composition, there is a notable increase COP by + 7.1 %, along with a decrease in VCC by −11.4 % and cooling capacity by 9.7 %.

Similarly, for the R-290/R-600 mixture, the same composition of 10/90 % has been identified as the “optimum”. This composition achieves the maximum COP (+11. 7 % compared to isobutane) and incurs relatively modest reductions in VCC and $\dot{Q}_o$ (-11.6 % and −7.5 %, respectively).

The calculated uncertainty for the three parameters determined for R-600a is less than 3.8 %. For the R-152/R-600 and R-290/R-600 mixtures, the average uncertainty is 3.9 %, with all compositions and parameters having uncertainties less than 4.2 %. It is important to note that none of the parameter values calculated during the composition evolution of the mixtures fall within the uncertainty region of R-600a.

It is important to emphasize that this choice has been done taking into account the authors’ opinion and based on quantitative and qualitative decisions, since it is difficult to unite all three parameters into one that designates which is the “best” composition.

The authors acknowledge that the determination of the “optimum” composition can be subject to debate and may vary depending on the specific application. Different researchers may hold differing opinions on what constitutes the ideal composition. However, it is essential to note that while selecting the right “optimum” composition may appear crucial, the values around these compositions exhibit similarity, and minor fluctuations in proportions would not significantly affect the overall performance of the system. In any case, these compositions have been chosen by the authors as the most favorable options based on their evaluation, considering the trade-offs and objectives at hand.

4.2. *Thermodynamic analysis of the “optimum” compositions*

4.2.1. *Phase change temperatures and glide*

Fig. 9 represents the evolution of the refrigerant temperature within both the condenser and the evaporator for the isobutane, R-152a/R-600 (10/90)% and R-290/R-600 (10/90)% at the “optimization” conditions ($t_{w,in}$ = 30 °C and $t_{gly,in}$ = 0 °C). Each heat exchanger is equipped with immersion thermocouples at 23.5 cm intervals along the pipe (which corresponds to an area of 46.88 cm^2 for the condenser and 70.32 cm^2 for the evaporator). This configuration enables a total of 16 temperature data points for the condenser and 15 for the evaporator, facilitating a detailed analysis based on direct measurements of their respective thermal evolutions.

In the condenser, two different regions can be differentiated. Initially, there is a pronounced temperature decrease, attributed to the desuperheating process that involves the removal of sensible heat from the vapor after the compression is completed, up to the point where condensation begins. Generally, this process finishes at the 3rd thermocouple, marked by a transition in the temperature trend, resulting in a smoother slope. This phase corresponds to the extraction of latent heat during the condensation process, persisting until the end of the condenser. It is noteworthy that no subcooling occurs, probably due to the use of a liquid vessel at the outlet condenser.

A comparable pattern is evident in the evolution of evaporator temperatures. The refrigerant enters the evaporator in two-phase state, which persists until the 12th thermocouple, at which point there is a notable shift in the temperature trend. This abrupt change signifies the beginning of superheating.

Fig. 9 shows the evolution of the three refrigerants tested. It must be noted that all along the condenser there is a pressure drop of 102 mbar for the R-600a, 60 mbar for the R-152a/R-600 (10/90)% and 62 mbar for R-290/R-600 (10/90)%, being 68 mbar, 64 mbar and 54 mbar in the evaporator respectively. The differences in these values compared to isobutane and the two mixtures, especially in the condenser, can be attributed to variations in mass flow, primarily due to isobutane’s higher density (as seen in Table 1). Specially in the evaporator, observing the isobutane temperature pattern, it suggests that the pressure drop mainly occurs in the initial part of the heat exchanger, as initially a decrease of the temperature is observed, which stabilizes latter in the process.

In the condenser, the phase-change temperature ($\bar{t}_k$), calculated as the mean temperature of the thermocouples within the two-phase zone, is 40.19 °C for the R-600a (at an average pressure of 5.45 bar), 37.83 °C for the R-152a/R-600 (10/90)% (4.64 bar) and 38.17 °C for the R-290/R-600 (10/90)% (at 4.44 bar). The evaporation temperature ($\bar{t}_o$), evaluated equally as the condensing temperature, shows a value of −9.67 °C for R-600a (at 1.16 bar), −9.13 °C for the R-152a/R-600 (10/90)% (at 0.92 bar) and −9.23 °C for the R-290/R-600 (10/90)% (at 0.9 bar).

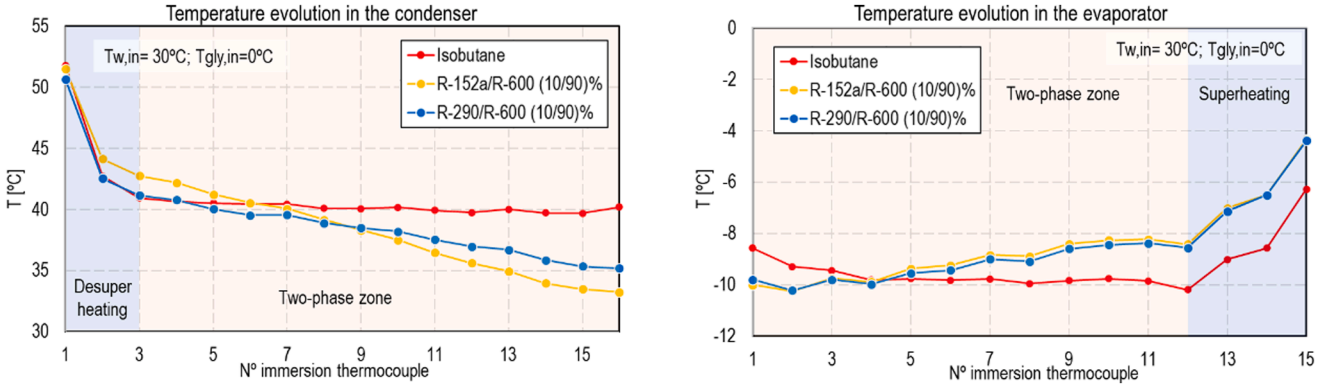

Fig. 9. Refrigerant temperature evolution in the condenser (left) and in the evaporator (right) of the three refrigerants tested.

While the evaporation temperatures are similar among the evaluated fluids, the condensing one presents lower values for the alternative mixtures, being the difference between both temperatures lower with the mixtures than with R-600a. This could contribute to a reduction on the compressor ratio expected and partly explain the COP increment seen with the alternative mixtures.

Reading the temperature difference between the starting and ending of the phase-change process (Δt_{pc}), two factors contribute to it: the pressure drop and the glide. The existing pressure drop, despite not presenting high values, may be significant, especially in the evaporator. R-600a exhibits a measured $\Delta t_{pc,k}$ of 0.76 K and a measured $\Delta t_{pc,o}$ of 1.62 K. Interestingly, and differently that happens whit the two alternative mixtures, these values align closely with those predicted by REFPROP (0.72 K and 1.55 K), supporting the authors' hypothesis of relying on direct measurements when feasible. For the two mixtures, the primary contribution to Δt_{pc} is attributed to their glide in addition to the pressure drop effect being cumulative for the condenser and subtractive for the evaporator. The mixture R-152a/R-600 (10/90)% present a measured $\Delta t_{pc,k}$ of 9.51 K and a $\Delta t_{pc,o}$ of −1.58 K, while for the mixture R-290/R-600 (10/90)% of 5.98 K and −1.23 K, respectively.

The two fluids with glide follow the typical glide temperature evolution, where the temperature variation is higher at lower vapor quality and diminishes as the vapor proportion increases. This could explain the different values between the glide measured in the condenser and in the evaporator, since while in the condenser the entire glide is measured, in the evaporator only the effective glide is, as the inlet is in a two-phase state, skipping the zone with the most significant temperature variations.

Table 3 provides comprehensive data, including evaporation and condensation temperatures as well as Δt_{pc} values for all the compositions considered, including butane. It's noteworthy that butane exhibits a higher evaporation temperature compared to isobutane (-7.94 °C at 0.82 bar). In contrast, the two alternative mixtures experience a reduction in temperature as the proportion of the lesser proportion refrigerant increases. This temperature reduction may be attributed to a decrease in the overall heat transfer coefficient, a characteristic feature of the mixtures. A similar trend can be observed in the condensing temperature, where butane displays a lower temperature than isobutane (37.86 °C at 3.64 bar). However, unlike the evaporation temperature, the fluctuations in temperature with changing compositions are less pronounced in the condenser, with all values remaining below that of isobutane.

In the supplementary information, the evolution of the temperature of the exchangers of the rest of the tests is available to represent their evolution, as well as the recorded pressures.

4.2.2. *Compressor power consumption and mass flow rate*

The evolution of the refrigerant mass flow and the compressor electric power use when varying the composition is presented in Fig. 10.

The mass flow rate of butane is lower than that of isobutane, with values of 5.69 kg·h^{-1} and 4.25 kg·h^{-1}, respectively. Presenting a lower density has the advantage that the power required for the compression is lower but, for a given volume, the mass flow circulating is lower, requiring higher compression volumes to satisfy the same cooling capacities. As the proportion of the secondary fluid increases in the mixture, the mass flow rate also increases, as expected, since the density increases accordingly. Interestingly, the mixture containing R-152a exhibits a higher mass flow rate than the one with R-290. This unexpected result may be attributed to the fact that the evaporation temperature is higher with R-152a for the same composition than with R-290. It could be also related to better volumetric efficiency characteristics of the mixture with R-152a.

The trend in $\dot{P}_c$ evolution follows a similar pattern to that observed in Volumetric Cooling Capacity (VCC) and Cooling Capacity ($\dot{Q}_o$). As the refrigerant mass flow rate increases, $\dot{P}_c$ also increases. It is worth noting that for all the compositions tested, the power consumption is lower than that required by R-600a. Specifically, R-600a exhibits a $\dot{P}_c$ of 173.4 W. In contrast, at the "optimum" compositions, the mixture R-152a/R-600 (10/90)% demonstrates an energy reduction of 15.7 %, while the R-290/R-600 (10/90)% mixture achieves an even greater reduction of 17.2 %.

5. Optimum compositions at varying temperature conditions

Finally, the "optimum" compositions were evaluated under different inlet secondary fluid temperatures. Fig. 11, Fig. 12. and Fig. 13 show the evolution of the COP, VCC and $\dot{Q}_o$ respectively of the R-600a, R-152a/R-600 (10/90)% and R-290/R-600 (10/90)%, together with the percentage increment of each test of the alternative mixtures with respect to the equivalent with isobutane. Three different water inlet and three different glycol inlet temperatures are considered, giving as a result nine different conditions.

The two considered mixtures exhibit significant increments in COP compared to isobutane in all tested points. Notably, the mixture R-290/R-600 (10/90)% outperforms the mixture R-152a/R-600 (10/90)% in terms of COP improvements. On average, R-290/R-600 (10/90)% demonstrates a 10.32 % increase across the 9 test cases, with percentage increments ranging from + 12.5 % (at $t_{gly,in} = 0$ °C and $t_{w,in} = 25$ °C) to 9.0 % (at $t_{gly,in} = 5$ °C and $t_{w,in} = 25$ °C). Conversely, R-152a/R-600 (10/90)% achieves an average increase of 7.31 %, with fluctuations between 9 % (at $t_{gly,in} = 5$ °C and $t_{w,in} = 35$ °C) and 6.1 % (at $t_{gly,in} = -5$ °C and $t_{w,in} = 35$ °C).

A similar trend is observed for the other two considered parameters, with both mixtures generally showing percentage reductions compared to R-600a. Notably, these reductions tend to be more pronounced in the case of the R-152a/R-600 (10/90)% mixture. Specifically, in terms of VCC, the propane mixture exhibits an average reduction of −8.8 %

Table 3
Summary of the reference test conditions, various thermodynamic aspects and energy parameters during the optimization process.

	Reference parameters					High pressure cycle section				Low pressure cycle section				Compression process				Energy parameters			
Refrigerant and mass composition	$t_{w,k,in}$ (°C)	$t_{gly,o,in}$ (°C)	$\dot{V}_{w,k}$ (L/h)	$\dot{m}_{gl,o}$ (kg/h)	Ref. charge (g)	$p_{k,in}$ (bar)	$p_{k,out}$ (bar)	$\bar{t}_k$ (°C)	$\Delta t_{pc,k}$ (°C)	$p_{o,in}$ (bar)	p_{suc} (bar)	$\bar{t}_o$ (°C)	$\Delta t_{pc,o}$ (°C)	p_{dis} (bar)	t_{dis} (°C)	C_r (-)	m_{ref} (kg/s)	P_c (W)	Q_o (W)	COP (-)	VCC (kJ/m^3)
R-600a																					
	30.02	−0.05	90.23	80.68	160	5.50	5.40	40.19	0.76	1.19	1.12	−9.67	1.62	5.60	59.66	4.98	5.69	173.4	435.9	2.51	827.4
R-600																					
	30.03	0.01	90.16	79.82	154	3.68	3.61	37.86	0.71	0.85	0.79	−7.94	1.44	3.75	59.34	4.75	4.25	133.6	360.8	2.74	640.4
R-152a/R-600																					
2.5/97.5	29.95	0.04	89.72	79.78	155	3.87	3.81	37.97	3.97	0.86	0.80	−8.26	0.66	3.93	60.13	4.93	4.25	134.4	371.3	2.76	657.9
5/95	30.01	0.03	89.93	79.53	141	4.18	4.12	37.77	6.91	0.89	0.83	−8.64	−0.44	4.24	61.08	5.11	4.34	137.2	379.2	2.76	686.3
7.5/92.5	29.92	0.01	89.77	79.54	146	4.37	4.31	37.80	8.25	0.90	0.84	−8.87	−0.88	4.43	62.15	5.28	4.46	142.6	388.8	2.73	696.5
10/90	**30.00**	**0.02**	**90.35**	**80.85**	**150**	**4.66**	**4.61**	**37.83**	**9.51**	**0.95**	**0.89**	**−9.13**	**−1.58**	**4.72**	**63.39**	**5.29**	**4.57**	**146.2**	**393.7**	**2.69**	**733.2**
12.5/87.5	29.98	0.01	89.90	79.52	152	5.02	4.96	37.68	11.00	0.96	0.89	−9.53	−2.79	5.06	64.09	5.68	4.56	148.9	397.5	2.67	743.7
15/85	30.00	−0.01	90.08	80.02	153	5.19	5.13	37.69	11.18	0.98	0.91	−9.61	−3.09	5.24	65.14	5.74	4.66	150	399.1	2.66	750.8
17.5/82.5	30.03	0.04	90.25	79.74	154	5.52	5.46	37.74	11.84	1.01	0.95	−9.93	−4.09	5.56	65.87	5.88	4.75	154.2	410.4	2.66	785.7
20/80	30.00	0.01	89.95	80.40	150	5.70	5.62	37.70	10.65	1.10	1.03	−9.36	−3.84	5.78	68.38	5.62	5.15	165.5	438.5	2.65	845.4
R-290/R-600																					
2.5/97.5	29.98	0.00	90.20	79.71	160	3.89	3.83	38.03	2.64	0.85	0.80	−8.57	0.70	3.95	60.57	4.93	4.29	137.6	379.5	2.76	662.7
5/95	29.96	0.00	90.29	80.10	140	3.96	3.89	37.84	3.17	0.88	0.83	−8.46	0.41	4.03	60.79	4.88	4.35	139.1	379.1	2.73	667.6
7.5/92.5	29.96	−0.03	90.06	80.09	147	4.27	4.21	38.11	5.16	0.90	0.85	−9.13	−0.65	4.33	61.58	5.09	4.35	141.4	394.6	2.79	710.4
10/90	**29.98**	**0.00**	**89.72**	**80.14**	**150**	**4.47**	**4.40**	**38.17**	**5.98**	**0.93**	**0.88**	**−9.23**	**−1.23**	**4.53**	**62.12**	**5.17**	**4.41**	**143.6**	**403.2**	**2.81**	**731.3**
12.5/87.5	29.96	0.02	89.87	80.03	152	4.71	4.65	38.23	6.92	0.96	0.91	−9.58	−1.92	4.76	63.15	5.26	4.49	146.1	408.4	2.80	747.3
15/85	29.98	0.02	90.01	80.01	154	4.93	4.87	38.29	7.84	0.98	0.93	−9.85	−2.56	4.98	63.26	5.37	4.46	149.3	416.7	2.79	778.9
17.5/82.5	29.97	0.05	89.72	80.23	154	5.19	5.13	38.56	8.52	1.01	0.95	−10.18	−3.16	5.24	64.83	5.50	4.59	155.4	433.6	2.79	803.4
20/80	29.95	0.00	89.63	79.43	150	5.35	5.29	38.57	8.89	1.03	0.97	−10.32	−3.46	5.40	64.79	5.54	4.61	156.2	435.9	2.79	818.1
22.5/77.5	29.98	−0.03	90.31	80.09	152	5.61	5.55	38.75	9.39	1.06	1.00	−10.58	−3.98	5.66	65.79	5.67	4.71	161.7	449.1	2.78	839.8
25/75	30.06	0.06	90.42	79.50	148	6.00	5.93	38.99	9.74	1.12	1.05	−10.85	−4.65	6.05	66.99	5.74	4.92	170.5	470.2	2.76	881.6

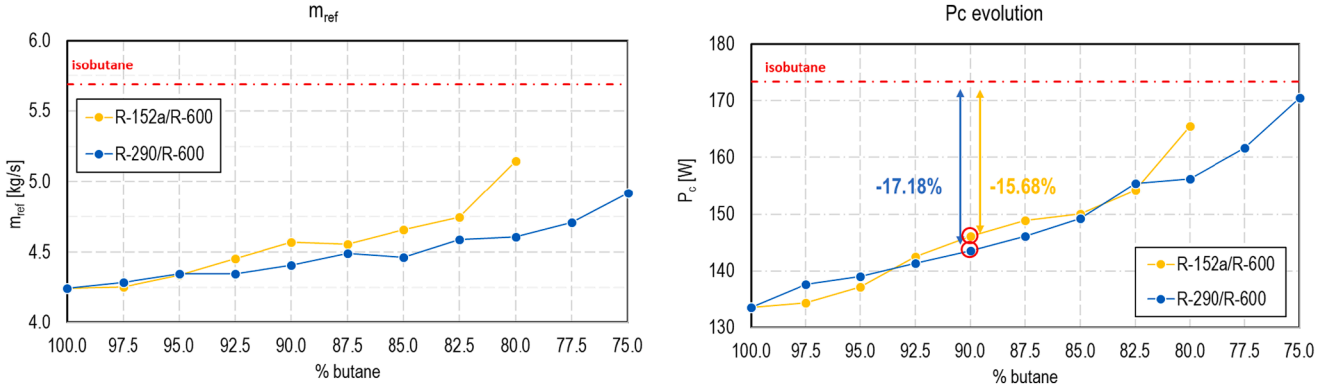

Fig. 10. Evolution of the refrigerant mass flow (left) and $\dot{P}_c$ (right) when varying the composition of the alternative mixtures. The m_{ref} and $\dot{P}_c$ obtained with isobutane are represented by the red line.

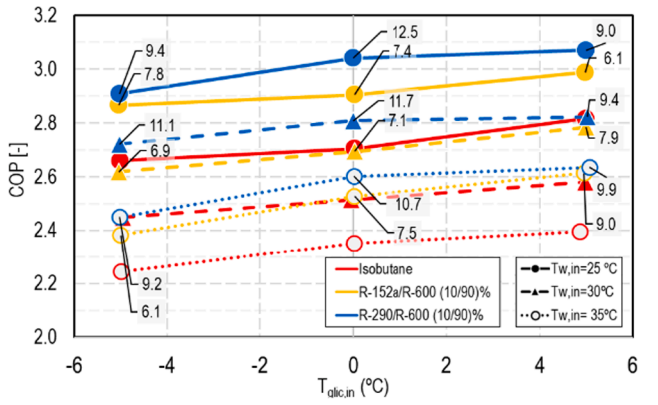

Fig. 11. COP evolution of the R-600a, R-152a/R-600 (10/90)% and R-290/R-600 (10/90)% at different inlet secondary fluid temperatures. Additionally, labels indicating the percentage increase relative to the equivalent R-600a test for the alternative mixtures are included. These labels are organized in pairs, with the upper label corresponding to R-290/R-600 and the lower one to R-152a/R-600.

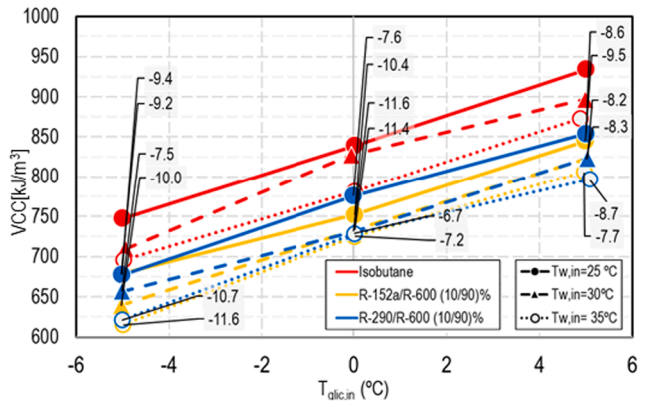

Fig. 12. VCC evolution of the R-600a, R-152a/R-600 (10/90)% and R-290/R-600 (10/90)% at different inlet secondary fluid temperatures.

(ranging from −10.7 % to −6.7 %), while the R-152a-containing mixture shows an average reduction of −9.5 % (ranging from −11.6 % to −7.2 %). Regarding $\dot{Q}_o$ values, the observed average reductions are −6.6 % (ranging from −8.7 % to −4.9 %) and −8.9 % (ranging from −11.4 % to −7%) for the two mixtures, respectively.

In summary, the results presented in this section corroborate the

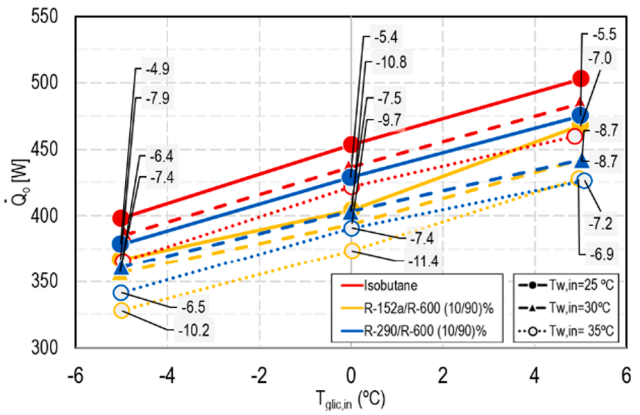

Fig. 13. $\dot{Q}_o$ evolution of the R-600a, R-152a/R-600 (10/90)% and R-290/R-600 (10/90)% at different inlet secondary fluid temperatures.

findings from the "optimization" process, highlighting a substantial COP improvement in the alternative mixtures compared to isobutane, with R-290/R-600 (10/90)% showing superior energy performance, regardless of external conditions. No clear patterns emerge to suggest that any mixture exhibits better performance under specific conditions, indicating a relatively consistent performance across different scenarios. It can be concluded that, in terms of energy performance, the R-290/R-600 (10/90)% mixture is a preferable alternative to R-152a/R-600 (10/90)% as a an alternative for R-600a, considering also that the both refrigerants constituting this mixture are natural.

The supplementary information contains a table analogous to Table 3, presenting the most important thermodynamic parameters of the mixtures discussed in this section under varying conditions.

6. Conclusions

In this study, an experimental optimization of the composition of the mixtures R-152a/R-600 and R-290/R-600 was conducted as an alternative to isobutane (R-600a) in a simple vapor compression cycle. A novel heat exchanger design, based on a tube-in-tube configuration with immersion thermocouples, was employed to monitor the refrigerant temperature evolution during the phase-change process.

The methodology involved testing all possible mass composition combinations of the two considered mixtures in steps of 2.5 %, ranging from 2.5 % to 20 % of R-152a (resulting in a total of 8 different mass compositions) and from 2.5 % to 25 % of R-290 (10 compositions). Results were compared to those obtained with R-600a under fixed boundary conditions. These conditions included an inlet water

temperature of 30 °C, an inlet glycol temperature of 0 °C, a water flow rate of 90 kg·h^{-1}, and a glycol flow rate of 80 kg·h^{-1}.

At those conditions, R-600a demonstrated a COP of 2.51, a VCC of 827.4 kJ·m^{-3}, and a $\dot{Q}_o$ of 435.9 W. In comparison, R-600 exhibited values of 2.74, 640.4 kJ·m^{-3}, and 366.25 W, respectively. The mixture R-152a/R-600 achieved the highest COP values at compositions of 2.5/97.5 % and 5/95 % (2.76), with a slight decrease as the R-152a composition increased. Similarly, the mixture R-290/R-600 reached its maximum COP at a composition of 10/90 % (2.81), maintaining a similar value until the proportion reached 20/80 %, after which it decreased. VCC and $\dot{Q}_o$ increased linearly as the secondary fluid proportion increased. R-152a/R-600 surpassed R-600a's VCC and $\dot{Q}_o$ values at a composition of (20/80)%, whereas R-290/R-600 did so at (22.5/77.5)% and (20/80)%, respectively.

The "optimum" compositions were chosen as (10/90)% for both mixtures, striking a balance between the three parameters. The mixture R-152a/R-600 (10/90)% exhibited a COP increase of + 7.1 %, with a decrease in VCC by −11.4 % and cooling capacity by −9.7 %. The mixture R-290/R-600 (10/90)% showed a COP increase of + 11. 7 %, along with a decrease in VCC by −11.6 % and cooling capacity by −7.5 %.

At these compositions, the R-152a-containing mixture presented an average condensing temperature of 37.8 °C at 4.64 bar, with a measured glide of 9.5 K. In the evaporator, the phase change temperature was −9.1 °C at 0.92 bar, with an effective glide of 1.6 K. The mixture R-290/R-600 (10/90)% exhibited condensing conditions of 38.2 °C at 4.4 bar, with a glide of 5.98 K, and evaporating conditions of −9.2 °C at 0.91 bar, with an effective glide of 1.2 K. As a reference, R-600a had condensing and evaporating temperatures of 40.2 °C and −9. 7 °C, respectively.

Furthermore, the performance of the "optimum" compositions was tested under nine different secondary fluid inlet temperatures, resulting in average increments and reductions compared to isobutane in the nine tests as follows:

- R-152a/R-600 (10/90)%: +7.3 % of COP, −9.45 % of VCC, and −8.9 % of $\dot{Q}_o$.
- R-290/R-600 (10/90)%: +10.3 % of COP, −8.77 % of VCC, and −6.6 % of $\dot{Q}_o$.

In summary, R-290/R-600 (10/90)% exhibits superior energy performance compared to R-152a/R-600 (10/90)% as an alternative for R-600a. R-290/R-600 (10/90)% can be considered as an interesting long-term alternative to R-600a, since the energy improvements respect to isobutane are significant, its thermodynamic properties are similar to those of R-600a and the two refrigerants constituting this mixture are natural.

7. Declaration of Generative AI and AI-assisted technologies in the writing process

During the preparation of this work the authors used "OpenAI. (2023). ChatGPT 3.5" in order to improve language and readability. After using this tool/service, the authors reviewed and edited the content as needed and take full responsibility for the content of the publication.

CRediT authorship contribution statement

Daniel Calleja-Anta: Conceptualization, Investigation, Methodology, Writing – original draft. **Manel Martínez-Ángeles:** Investigation, Writing – review & editing. **Laura Nebot-Andres:** Writing – review & editing. **Daniel Sánchez:** Conceptualization, Investigation, Methodology, Writing – original draft. **Rodrigo Llopis:** Conceptualization, Funding acquisition, Supervision, Writing – review & editing.

Declaration of competing interest

The authors declare that they have no known competing financial interests or personal relationships that could have appeared to influence the work reported in this paper.

Data availability

No data was used for the research described in the article.

Acknowledgments

Authors gratefully acknowledge for the economic support to this study to Jaume I University (grant PREDOC/2019/19). This article is part of the project TED2021-130162B-I00, funded by MCIN/AEI/10.13039/501100011033 and by the European Union - NextGenerationEU "NextGenerationEU"/PRTR.; and of the project PID2021-126926OB-C21 funded by the Ministerio de Ciencia e Innovación of Spain.

Appendix A. Supplementary material

Supplementary material to this article can be found online at https://doi.org/10.1016/j.applthermaleng.2024.123070.

References

[1] European Commission, 2014. Regulation (EU) No 517/2014 of the European Parliament and of the Council of 16 April 2014 on fluorinated greenhouse gases and repealing Regulation (EC) No 842/2006., in: Commission, E. (Ed.), Official Journal of the European Union.
[2] UNEP, 2018. Refrigeration and air conditioning and heat pumps technical options committee. 2018 Assessment Report. United Nations Environment Programme, Kenya.
[3] International Electrotechnical Commission., 2019. IEC 60335-2-89:2019. Household and similar electrical appliances - Safety - Part 2-89: Particular requirements for commercial refrigerating appliances and ice-makers with an incorporated or remote refrigerant unit or motor-compressor.
[4] IPCC, 2023. Climate Change 2023: Synthesis Report. Contribution of Working Groups I, II and III to the Sixth Assessment Report of the Intergovernmental Panel on Climate Change [Core Writing Team, H. Lee and J. Romero (eds.)]. IPCC, Geneva, Switzerland, pp. 35-115.
[5] M. Rasti, S. Aghamiri, M.-S. Hatamipour, Energy efficiency enhancement of a domestic refrigerator using R436A and R600a as alternative refrigerants to R134a, Int. J. Therm. Sci. 74 (2013) 86–94.
[6] D. Sánchez, A. Andreu-Nácher, D. Calleja-Anta, R. Llopis, R. Cabello, Energy impact evaluation of different low-GWP alternatives to replace R134a in a beverage cooler. experimental analysis and optimization for the pure refrigerants R152a, R1234yf, R290, R1270, R600a and R744, Energy Conver. Manag. 256 (2022).
[7] E. Granryd, I. Ekroth, P. Lundqvist, A. Melinder, B. Palm, P. Rohlin, Refrigerating engineering, Royal Institute of Technology, KTH, Department of Energy Technology, Division of Applied Thermodynamics and Refrigeration, 2009.
[8] D. Sánchez, R. Cabello, R. Llopis, I. Arauzo, J. Catalán-Gil, E. Torrella, Energy performance evaluation of R1234yf, R1234ze(E), R600a, R290 and R152a as low-GWP R134a alternatives, Int. J. Refrig. 74 (2017) 269–282.
[9] Ashrae, ANSI/ASHRAE Standard 34–2019, American Society of Heating, Refrigerating and Air-Conditioning Engineers Inc, Atlanta, USA, Designation and safety classification of refrigerants, 2019.
[10] C. Aprea, A. Greco, A. Maiorino, An experimental investigation on the substitution of HFC134a with HFO1234YF in a domestic refrigerator, Appl. Therm. Eng. 106 (2016) 959–967.
[11] C. Aprea, A. Greco, A. Maiorino, C. Masselli, A. Metallo, HFO1234ze as drop-in replacement for R134a in domestic refrigerators: an environmental impact analysis, Energy Procedia 101 (2016) 964–971.
[12] B.O. Bolaji, Experimental study of R152a and R32 to replace R134a in a domestic refrigerator, Energy 35 (2010) 3793–3798.
[13] A. Maiorino, C. Aprea, M.G. Del Duca, R. Llopis, D. Sánchez, R. Cabello, R-152a as an alternative refrigerant to R-134a in domestic refrigerators: an experimental analysis, Int. J. Refrig. 96 (2018) 106–116.
[14] M. Mohanraj, S. Jayaraj, C. Muraleedharan, P. Chandrasekar, Experimental investigation of R290/R600a mixture as an alternative to R134a in a domestic refrigerator, Int. J. Therm. Sci. 48 (2009) 1036–1042.
[15] D. Calleja-Anta, L. Nebot-Andres, J. Catalan-Gil, D. Sánchez, R. Cabello, R. Llopis, Thermodynamic screening of alternative refrigerants for R290 and R600a, Results in Engineering (2020) 5.

[16] D. Calleja-Anta, L. Nebot-Andres, D. Sánchez, R. Cabello, R. Llopis, Drop-in substitutes for R-600a. Experimental evaluation and optimization of a commercial fridge, Appl. Therm. Eng. 211 (2022).
[17] D. Calleja-Anta, D. Sánchez, L. Nebot-Andrés, R. Cabello, R. Llopis, Alternative mixtures to R-600a. theoretical assessment and experimental energy evaluation of binary mixtures in a commercial cooler, Int. J. Refrig 152 (2023) 83–92.
[18] E.W. Lemmon, I.H. Bell, M.L. Huber, M.O. McLinden, NIST standard reference database 23: reference fluid thermodynamic and transport properties-REFPROP, version 10.0, Nat. Inst. Standards Technol. (2018).
[19] Conde, M., 2011. Thermophysical properties of brines.
[20] O. Kunz, W. Wagner, The GERG-2008 wide-range equation of state for natural gases and other mixtures: an expansion of GERG-2004, J. Chem. Eng. Data 57 (2012) 3032–3091.
[21] I.H. Bell, E.W. Lemmon, Automatic fitting of Binary Interaction Parameters for multi-fluid helmholtz-energy-explicit mixture models, J. Chem. Eng. Data 61 (2016) 3752–3760.
[22] D. Calleja-Anta, L. Nebot-Andres, R. Cabello, D. Sánchez, R. Llopis, A3 and A2 refrigerants: border determination and hunt for A2 low-GWP blends, Int. J. Refrig 134 (2022) 86–94.